# Calibration and survey of AMANDA with SPASE

**X. Bai[1], R. Engel[1], T. K. Gaisser[1], J.A. Hinton[2], A. Karle[3], M. Kowalski[4], D. Martello[5], T. Miller[6], K. Rawlins[3], K. Rochester[2], G. M. Spiczak[1], T. Stanev[1], A. A. Watson[2], and the AMANDA Collaboration[7]**

[1]Bartol Research Institute, Univ. of Delaware, Newark, DE 19716, USA

[2]Dept. of Physics, University of Leeds, LS2 9JT, Leeds, U.K.

[3]Dept. of Physics, University of Wisconsin, Madison, WI 53706, USA

[4]DESY-Zeuthen, Germany

[5]INFN, Lecce, Italy

[6]Applied Physics Lab, Baltimore, MD 20723, USA

[7]Complete author list is found at the end of this volume

**Abstract.** We report on analysis of coincident observation of air showers by the South Pole Air Shower Experiment (SPASE) and the Antarctic Muon and Neutrino Detector Array (AMANDA). We emphasize the response of AMANDA to muon bundles and the use of coincident events for calibration and survey of the deep AMANDA detector. This analysis is confined to data taken during 1997 when both SPASE-1 and SPASE-2 were in operation.

## 1  Introduction

The presence of SPASE on the surface provides a set of externally tagged muon bundles that can be measured by AMANDA. Such measurements allow a study of the response of AMANDA that is complementary to studies of the deep detector with atmospheric muons and neutrinos, internal calibration sources and Monte Carlo simulations. In addition it makes possible a muon survey of AMANDA optical module (OM) locations and ice properties that complements internal assessments.

Figure 1 shows a plan view of the physical configuration of the three detectors in 1997, during which the data reported here were collected. That season was the first for AMANDA B10 (Wiebusch for the AMANDA Collaboration, 2001) and the last for SPASE-1 (Smith *et al.*, 1989; Beaman *et al.*, 1993; van Stekelenborg *et al.*, 1993), which was removed in December, 1997. Having two surface arrays gave a unique stereo view of the deep detector. In this paper we discuss the calibration and survey aspects of the SPASE-AMANDA data. Analysis of coincident events to determine composition is underway and will be the subject of a future publication.

## 2  The SPASE-AMANDA telescopes

Both SPASE-1 and SPASE-2 (Dickinson *et al.*, 2000) are scintillator arrays on a 30 m triangular grid, enclosing areas

*Correspondence to:* gaisser@bartol.udel.edu
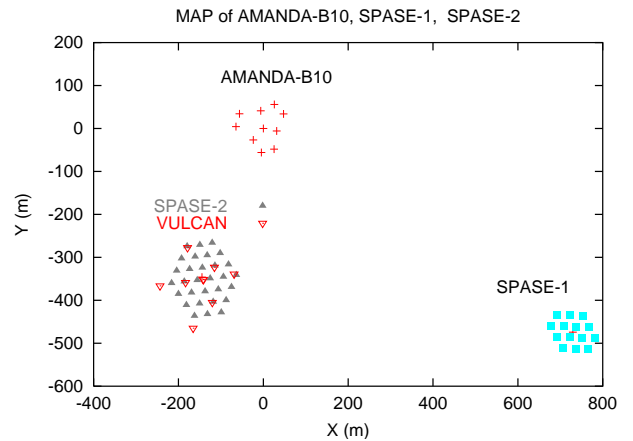


**Fig. 1.** Map showing locations of SPASE-1 and SPASE-2 relative to locations of AMANDA-B10 strings at the surface. The origin of the AMANDA coordinate system is near string 4, and the plus-Y direction is grid-north. Azimuth is measured counter-clockwise from grid-east. Thus the center of SPASE-2 is at $247°$ and the center of SPASE-1 is at $327°$.

of 6000 and 16000 m$^2$ respectively. The 302 OMs in B10 form an instrumented cylinder of ice approximately 400 m high and 120 m in diameter. A line from the center of B10 to the center of SPASE-2 has a zenith angle of $12°$. The corresponding angle to SPASE-1 is $26°$. The combination of either surface array with AMANDA constitutes a cosmic-ray detector with an acceptance of

$$\mathcal{A} \approx \frac{A_S \cos\theta \times A_{S-B10}}{d^2} = \Delta\Omega \times A_{S-B10}, \qquad (1)$$

where $A_S$ is the area of the surface array and $A_{S-B10}$ is the projected area of B10 viewed from the surface array. The solid angles of the acceptance cones are small, $\Delta\Omega_1 \approx 0.0015$sr and $\Delta\Omega_2 \approx 0.005$sr. Given the dimensions listed above, $\mathcal{A}_1 \approx 50$ m$^2$sr and $\mathcal{A}_2 \approx 100$ m$^2$sr. These acceptances may be used to estimate the coincident rate by multiplying by the cosmic-ray flux above threshold
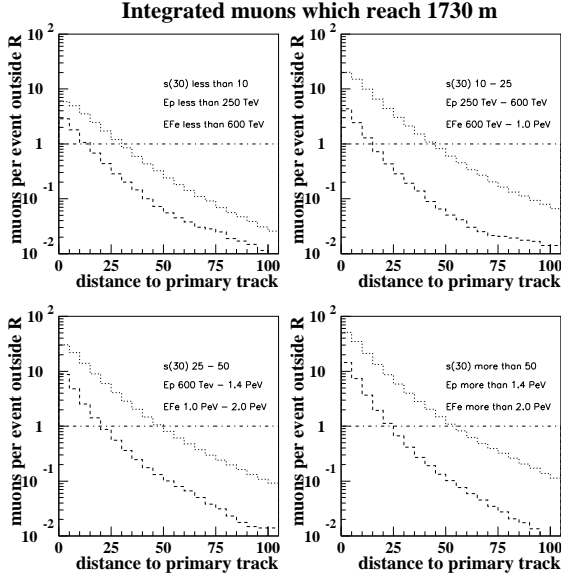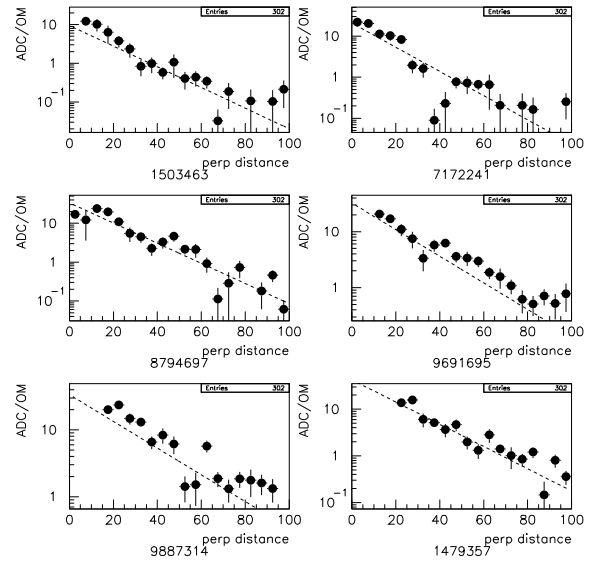
**Fig. 2.** Integral lateral distribution of muons at the depth of AMANDA for simulated proton (dashed) and iron (dotted) showers. The plot shows the average number of muons at distances larger than a given radius for the four $S_{30}$ intervals described in the text. The intercept at zero radius is the average muon multiplicity for that class of events.



**Fig. 3.** Lateral distribution of 6 events with energies in the PeV range as measured by AMANDA-B10.

for the air shower arrays, which become fully efficient above $\sim 200$ TeV. The coincidence rate for showers above this energy is $\sim 10^{-3}$ Hz.

The scintillator detectors of the surface arrays respond to passage of charged particles, mostly electrons and positrons and some low energy muons. The reconstructed particle density in the shower front at 30 m from the core ($S_{30}$) is used as a measure of shower size. Timing of the arrival of the shower front is used in the conventional way to reconstruct the arrival direction of each shower. With a 30 m grid spacing, the energy threshold for the SPASE arrays is about 30 TeV for proton-initiated showers, but the angular resolution is poor near threshold. The $\sigma$ of the direction reconstruction improves to about $2°$ at $S_{30} = 5$ ($\sim 150$ TeV for protons) and to $\approx 1°$ for showers with energy above 1 PeV (Dickinson *et al.*, 2000). In our analysis we group events into four large bins of $S_{30}$: $5 \leq S_{30} < 10$, $10 \leq S_{30} < 25$, $25 \leq S_{30} < 50$, and $S_{30} \geq 50$. The lowest-energy bin includes events with energies up to $\sim 300$ TeV, while the highest-energy bin is roughly the region of the knee (1-10 PeV).

## 3 Muon bundles in AMANDA

High energy muons in the shower core with sufficient energy at production propagate down through the ice and are visible in AMANDA for showers with trajectories within the acceptance cone. The minimum muon energy required to reach the top of B10 from SPASE-2 is about 370 GeV, and muons

with $E_\mu > 540$ GeV at production can penetrate through it. Since the lateral distribution of the muon bundles is determined primarily from the transverse momentum of pions at production 10-20 km above the ground, the muon bundles are characterized by a typical radius of $\sim 20$ m at the top of B10 and $\sim 10$ m at the bottom. About half of the muons that reach the top of B10 range out inside it. Simulations show that the typical number of muons per shower that reach the depth of the center of AMANDA are respectively 3, 5, 10 and 15 for proton induced showers in the four $S_{30}$ bins listed above. The corresponding numbers for showers generated by iron nuclei are a factor 2-3 greater. Simulation results for the average properties of muon bundles in AMANDA are shown in Fig. 2

For the study of muon bundles with AMANDA in coincidence with air showers measured by the surface array, it is desirable to determine the trajectory of the event as accurately as possible. With a $\sim 2°$ accuracy of the SPASE direction reconstruction, using the direction assigned by the surface array alone would lead to an uncertainty in locating the trajectory at AMANDA comparable to the lateral extent of the B10 detector itself. We therefore developed a method that uses the ADC information in AMANDA to define a core location at depth that is then connected with the SPASE core location on the surface to determine the trajectory. Fig. 3 shows examples of the measured ADC lateral distributions from light generated by six large muon bundles in AMANDA for which the trajectories were determined with this combined fit. Analysis is in progress to relate this information to the muon number and hence, in conjunction with the measurement of the surface showers, to determine on a statistical basis a measure of the primary composition up to and through

**Fig. 4.** Muon survey of AMANDA B10 (view from SPASE-1).
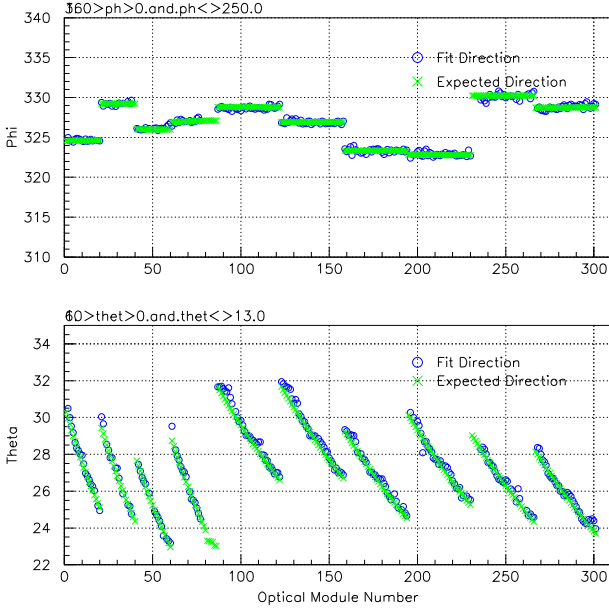


**Fig. 5.** Muon survey of AMANDA B10 (view from SPASE-2).

the region of the knee. In the remainder of this paper we focus on calibration and survey aspects.

## 4  Muon calibration and survey

Most, but not all, AMANDA modules face downward, in keeping with its primary function as a neutrino telescope. The detector nevertheless has good sensitivity to downward events, which is presumed to be a consequence of photon scattering in the refrozen hole-ice immediately surrounding the optical modules. Thus downgoing events can be used to calibrate the response of AMANDA to both downward and upward events.

### 4.1  Absolute pointing of AMANDA

Because air showers that trigger SPASE typically contain several muons with sufficient energy to reach the depth of AMANDA, the downward coincident events are in a different class from both single downgoing atmospheric muons and neutrino-induced upgoing muons. The standard AMANDA reconstruction method uses timing based on the assumption of a line source of Cherenkov light, i.e. the muon trajectory. For a muon bundle, however, the source of the light is intrinsically spread out over a typical diameter of roughly 30 m. This difference is a potential systematic limitation.

A straightforward measure of the absolute pointing accuracy of AMANDA is to compare the directions assigned by the AMANDA reconstruction algorithm for coincident events with the directions assigned independently by SPASE. During 1997, in addition to the two air shower arrays, the GASP atmospheric Cherenkov telescope (Barbagli *et al.*,
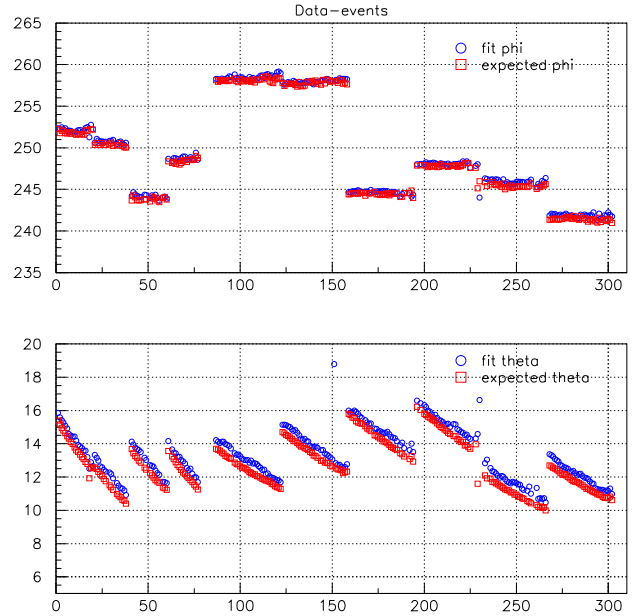
1993) was also running. Because the threshold of GASP for cosmic-ray showers is significantly lower than for the air shower detectors, GASP coincidences consist mostly of single muons at AMANDA. These events therefore have different systematics from SPASE events. Coincidences from all three independent experiments were used to check the pointing accuracy of AMANDA. All agree with each other in the average absolute pointing of AMANDA to within 1 to 2 degrees in sky coordinates. Using directions determined by the surface detectors as calibration standards, the pointing of the AMANDA event reconstruction was determined to be accurate to within half a degree in azimuth. There appears to be a small systematic offset in zenith of about $1.5°$. This is much smaller than the size of the AMANDA point source search bin of half angle $\approx 6°$. We note that these calibrations are for fixed zenith angles of $\approx 26°$ and $\approx 12°$.

### 4.2  Muon survey of B10

Two methods have been used to obtain a muon survey of AMANDA module locations. Both start from the zenith and azimuth of showers as determined by SPASE for events in which a particular OM in B10 is hit. In the first method, the fitted mean direction of events that trigger an OM is compared to the direction from the geometric center of SPASE to that OM. SPASE triggers have a steep distribution in zenith angle which biases the comparison when folded with the uncertainty in the SPASE reconstruction. To remove this bias, we divide the angular distribution for all hits on each OM by the angular distribution for all SPASE triggers. Fig. 4 shows the result for the survey of B10 from SPASE-1 using this method.

SPASE-2 is larger and closer to AMANDA than SPASE-1.

Thus the approximation underlying the first method (that every trajectory passes through the center of the surface array) introduces relatively bigger errors. We therefore adopted a second survey method in which the expected direction for each event was taken as the direction from the shower core at the surface (as determined by SPASE for the event) to the OM position as determined from the AMANDA survey, which consists of station survey, drill log data and internal laser calibrations. For each OM the distributions of apparent minus expected angle were fitted for zenith and azimuth separately. For SPASE-1 the results are indistinguishable from Fig. 4. The muon survey of SPASE-2 using this event-by-event method is shown in Fig. 5. The agreement with the nominal OM locations is within $\sim 0.5°$ in azimuth ($\sim 3$ m laterally), and there is a $0.5°$ systematic offset in zenith (bottom panel).

While the event-by-event method is better geometrically, the trigger biases mentioned above in connection with the steep zenith angle distribution have not been explicitly removed (though the apparent-minus-expected distributions for each OM are fitted to a Gaussian plus a background which is allowed to have a linear dependence on angle). To study these effects, we performed the same survey with simulated data. Showers were generated with a modified version of MOCCA (Hillas, 1995) using QGSJET (Kalmykov *et al.*, 1997) and SIBYLL (Fletcher *et al.*, 1994; Engel *et al.*, 1999) as hadronic interaction models (also including kaons as shower particles in MOCCA). High energy muons were propagated through the ice to the B10 detector and the AMANDA response was calculated. The simulations show essentially no offset in azimuth, as expected, while the average $0.5°$ offset in zenith is seen as in the data.

### 4.3 Ice properties

The same data can be used to obtain a measure of the effective attenuation length of the ice by comparing the response of OMs at different depths to showers as a function of impact parameter. OMs embedded in layers with more dust cannot see events from as far away as those in clearer layers. The impact parameter distribution of the hit probability for each OM is fit to an exponential over a limited range of impact parameters. Since the impact parameter for each event is determined by projecting the trajectory determined by SPASE, the impact parameter distribution is spread significantly compared to the true distribution. We have not attempted to deconvolve the SPASE angular resolution, so the "relative" attenuation length so determined is significantly larger than the true effective attenuation length as measured internally by AMANDA. Fig. 6 shows the relative attenuation length as a function of depth. The prominent features of this plot match up well with the properties of south pole ice as determined from completely independent methods (Price, 2000).

It is interesting to note that the zenith offset seen in the event-by-event analysis of SPASE-2 – B10 coincidences has a periodic dependence on OM number, which translates into a correlation with depth of the OMs. This is an interesting
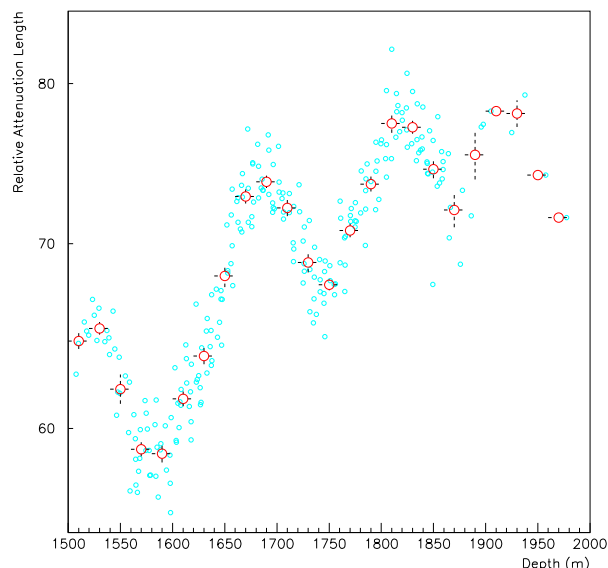


**Fig. 6.** Fit relative attenuation length vs. depth (see text).

second-order manifestation of ice properties that apparently reflects a bias for events passing above or below the modules depending on the clarity of the surrounding ice layers in which they are embedded. The effect at present shows up more sharply in the Monte Carlo than in the data. It should be possible to tune the treatment of ice properties in the Monte Carlo with this data–another illustration of the use of the SPASE-tagged muon beam for calibration of AMANDA.

### References

G. Barbagli *et al.* Nucl. Phys. (Proc. Suppl.) 32 (1993) 156.

J. Beaman *et al.*, Phys. Rev. **D48** (1993) 4495.

J.E. Dickinson *et al.*, Nucl. Instr. Meth. A **440** (2000) 95.

R. Engel, T.K. Gaisser, P. Lipari, and T. Stanev, Proc. Int. Cosmic Ray Conf. **1** (1999) 415, Salt Lake City, Utah.

R.S. Fletcher, T.K. Gaisser, P. Lipari, and T. Stanev, Phys. Rev. **D50** (1994) 5710.

A.M. Hillas, Proc. 24th Int. Cosmic Ray Conf. **1** (1981) 270, Rome, Italy.

N.N. Kalmykov, S. Ostapchenko, and A.I. Pavlov, Nucl. Phys. B (Proc. Suppl.) **52B** (1997) 17.

P. B. Price, K. Woschnagg, and D. Chirkin, Geophys. Res. Lett. **27** (2000) 2129.

N.J.T. Smith *et al.*, Nucl. Instr. Meth. A **276** (1989) 622.

J. van Stekelenborg *et al.*, Phys. Rev. **D48** (1993) 4504.

C. Wiebusch for the AMANDA Collaboration, "Observation of High Energy Atmospheric Neutrinos with AMANDA", this conference.